Robust Trajectory Planning in Person Following for Vision-based Autonomous Land Vehicle Guidance by Visual Field Model and Visual Contact Constraints

Ching-Heng Ku and Wen-Hsiang Tsai
Department of Computer and Information Science
National Chiao Tung University, Hsinchu, Taiwan 300, Republic of China
E-mail: gis82568@cis.nctu.edu.tw and whtsai@cis.nctu.edu.tw

Abstract

A robust trajectory planning for autonomous land vehicle (ALV) guidance in person following by a visual field model and visual contact constraints is proposed. The visual field model contains a visible area and a person-bounded area. When a vision-based ALV navigates by following a walking person in front, the person has to be detected from the image that is captured by a camera. Robust trajectory planning aims to guide the ALV to achieve the goal that the person always appears in the image when the ALV follows the person. It is found in this study that this goal can be achieved when three visual contact constraints in the visual field model are satisfied. The visual field model and the constraints are proposed according to the relation between the position of the visible area and that of the person-bounded area so that the optical axis of the camera points to the person. According to the visual contact constraints, a robust trajectory of the ALV can be derived. Besides, two theorems are proposed to show the robustness of the trajectory. According to the theorems, a maximum speed for generating a robust trajectory can be obtained. Finally, an algorithm of trajectory planning for ALV guidance is proposed to compute the turning angle of the next cycle for the front wheels of the ALV. This approach is implemented on a real ALV, and successful navigation sessions confirm the feasibility of the approach.

1. Introduction

In recent years, many approaches to autonomous land vehicle (ALV) guidance in indoor or outdoor environments are developed. These methods depend on the use of extracted features, such as lines[3][4], corners[5][6], models[7][8], roads[11][12], cars[13] [14], persons[15-17] or special landmarks[9][10]. In this study, the guidance of a vision-based ALV by a walking person ahead is our interest. This way of ALV guidance can lead the ALV to any place the person wants to reach, and this creates many possible applications. For example, the system can be used as an autonomous handcart, go-cart, buffet car, shopping car, golf cart, etc. Besides, The system can also be used as a learning system to collect information in certain environments, including open paths or locations with obstacles.

When the vision-based ALV navigates by following a walking person in front, the person has to be detected from the image that is captured by a camera. Our method for detecting the person and the organization of the ALV are introduced in detail in [1]. Although the image of the person is also detected in some pedestrian tracking systems [18-20], the image is acquired with a stationary CCD camera. In person following here, the location of the camera is moved according to the position of the ALV. When the relative position of the person to the ALV is calculated, a trajectory for the ALV need be generated to obtain a turn angle for the front wheels of the ALV. Some trajectory planning approaches [21-22] have been proposed. Munoz and Ollero [21] combined an original kinematic visibility graph planning method, a path generation algorithm based on beta-spline curves, and a cubic spline speed profile definition technique to propose a smooth trajectory planning method for mobile robots. Shiller and Serate [22] proposed a trajectory planning method for computing the track forces and track speeds of planar tracked vehicles required to follow a given path at specified speeds on horizontal and inclined planes. These methods do not generate a robust trajectory for a vision-based vehicle for following a person. The goal of this study is to propose a robust trajectory planning method to guide the ALV so that the person always appears in the image when the ALV follows the person. The flowchart of the proposed person following system is shown in Fig.1. In this study, we focus on the steps of trajectory planning and following.

A visual field model and three visual contact constraints for generating robust trajectories are proposed. The visual field model contains a visible area and a person-bounded area. When the visible area totally covers the person-bounded area, the person can be confirmed to appear in the captured image. According to the relation between the position of the visible area and that of the person-bounded area, three visual contact constraints are built. Furthermore, the formula of a trajectory for the ALV to follow the person smoothly according to the person's position is derived to satisfy the visual contact constraints. Two theorems showing the robustness of the derived trajectory for successional and smooth navigation are also derived. Finally, a trajectory planning algorithm is proposed. The algorithm makes the ALV keep visual contact with the person any time and keep a certain range of a distance from the person.

In the remainder of this paper, the proposed visual field model and visual contact constraints are presented in Section 2. According to the visual contact constraints, the formula of the proposed trajectory and limiting distances between the vehicle and the person are derived in Section 3. In Section 4, the two theorems to show the robustness of the trajectory are derived. According to the theorems, a maximum speed for generating a robust trajectory can be obtained. The proposed algorithm of trajectory planning is described in Section 5. In Section 6, experimental results are illustrated. Conclusions are included in the last section.

2. Proposed Visual field Model and Visual Contact Constraints

The proposed visual field model considers the visual field of the camera and the possible positions of the person who walks in front of the ALV. The camera mounted on the ALV is used to capture the image of the person and its visual field is bounded by the visual angle of the camera. If the person appears in the visual field of

the camera, the captured image will include the person. However, because the ALV cannot move with abrupt direction changes like the person, capturing the person in an image at one instant does not guarantee successful capture of the person at the next moment. Hence, the possible positions of the person at the next instant have to be included in the visual field of the camera. This condition can be formulated by the visual contact constraints proposed in Section 2.2. In Section 2.1, the definition of the visual field model is described first.

2.1. Definition of proposed visual field model

In our study, the direction of the optical axis of the camera is adjusted to be the same as that of the ALV head. Therefore, the person will appear in the image captured with the camera when he/she is on the straight head direction of the ALV. Furthermore, the relation between the direction of the optical axis and that of the front wheels can be obtained according to the relation between the direction of the ALV head and that of the front wheels.

The visual field model is composed of a visible area of the camera and a person-bounded area, as illustrated in Fig. 2. In the figure, the interior of the triangle is the visible area and the interior of the circle is the person-bounded area. Images are captured using a mounted camera on the vision-based ALV. The camera possesses a constant visual angle (the angle of 2α shown in Fig. 2). The value of the visual angle depends on the lens of the camera. Besides, the visual angle decides the visual field of the camera. The bigger the visual angle, the wider the visual field. As well known, a lens with a bigger visual angle is usually called a wide-angle lens. In this study, the visual angle of the camera is assumed to be known and used to determine the visible area. As shown in Fig. 2, the two vertical projection of the lines of sight whose intersection angle is the visual angle are called the left and the right boundary lines of the camera. The intersection of the left and the right boundary lines is the location of the camera. The visible area of the current ALV position B is defined as the area bounded by the left and right boundary lines which form the visual angle 2α of the camera, as shown in Fig. 2.

The person-bounded area is defined to be the one which covers all possible positions of the person away from the current one in the next time instant. The duration between two time instants is called a unit time and is defined as the time interval between two image samplings. Hence, the person's position in the next instant will be located inside the person-bounded area. Besides the current position and the unit time, the speed of the person also has to be considered to obtain all possible positions of the person. Because the speed and the direction of the person do not keep the same all the time, the possible positions are hard to predict strictly. However, we can cover all possible positions of the person by a circle. More specifically, as shown in Fig. 2, if the person walks from a position P to another position Q in a constant speed v for a certain time unit t, the position Q will form a circle whose center and radius are P and vt, respectively. The circle, denoted as $C_{p,v,t}$, is called the *person-bounded area* of P at speed v for time t.

2.2. Proposed visual contact constraints

Although the person detected from the image can be located at any place in the visible area, the next position of the person may be out of the visible area so that the person will not appear in the next captured image. In order to keep the person within the visible area, the visible area must cover the person-bounded area totally at any time. An illustration of the positions B and P of the ALV and the person, respectively, at two time instants are shown in Fig. 3, where the visible areas of B_i and B_{i+1} totally cover the person-bounded areas of P_i and P_{i+1}, respectively. According to the relation between the position of the visible area and the person-bounded area, three visual contact constraints to guarantee that the person always appears in the image are formulated in this study as follows:

$$A(B_i, P_i) \le \alpha \tag{1}$$

$$A(B_{i+1}, P_i) = 0 \tag{2}$$

$$d_1 \le D(B_{i+1}, P_i) \le d_2 \tag{3}$$

where B_i and B_{i+1} represents the current and the next position of the vehicle, respectively, P_i represents the current position of the person, A is the angle between the direction of the vehicle head and that from the vehicle to the person, D is the distance between the vehicle and the person, α is a half of the visual angle, and d_1 and d_2 are two limiting distances.

These three constraints are explained in detail in the following. The first constraint in (1) is the precondition of the other ones and guarantees that the person's position P_i is located in the visible area and appears in the captured image. When the visual angle of the camera is 2α, the angle between the direction of the vehicle head and that of the left or the right boundary of the visual area is α. Hence, the person's position P_i detected from the image makes the angle $A(B_i, P_i)$ smaller than α if the person appears in the image.

The second and third constraints in (2) and (3) describe the intended relation between B_{i+1} and P_i. The person's next position P_{i+1} is detected when the vehicle arrives at the next position B_{i+1}, so the position P_{i+1} is not considered in the current time instant. The second constraint in (2) says that the person's current position P_i is right on the straight direction of the vehicle head (i.e., the camera direction) at the next position B_{i+1} of the vehicle so that the angle $A(B_{i+1}, P_i)$ is zero. This constraint can be achieved according to the proposed trajectory described in the next section. Constraint (3) says that the distance between B_{i+1} and P_i must be bounded in a range (described in detail in Section 3.2) so that the person-bounded area of P_i is totally covered by the visible area of B_{i+1}. When these three constraints are satisfied, the person's next position P_{i+1} can be guaranteed to appear in the visible area of B_{i+1}. An analysis of the constraints is given in Section 4.

3. Formulas for Satisfying Visual Contact Constraints

3.1. Proposed method for deriving trajectory for satisfying the second visual contact constraint

The proposed method for deriving the trajectory which satisfies the second visual contact constraint proposed in the previous section is introduced in this section. Before deriving the trajectory, a model for the kinematic trajectory of the vehicle is introduced first. The model is the basis of our method. Using this model, the trajectory and the position of the vehicle in the next time instant can be obtained. The adopted kinematic model for an automobile with front and rear tires[2] is shown in Fig. 4. The rear wheels are aligned with the car while the front wheels are allowed to spin about the vertical axes. Besides, the center position between two front wheels is treated as the origin point of the coordinate system of the vehicle. This assumption is helpful in deriving the formula of the trajectory.

The kinematic trajectory of the vehicle is a circular curve. The position B is a certain point of the circular path and its coordinates are x and y. The values of x and y are

calculated as follows:

$$x = P \cos u \text{ and} \quad (4)$$
$$y = P \sin u, \quad (5)$$

where P is the straight distance from the origin point O to the point B and u is the angle between the X-axis and the vector from O to B. The values of x and y are expressed as the functions, as described in the following, of the turn angle and the speed of the vehicle. We assume that the vehicle travels a distance S from the origin point O to the point B by turning an angle of δ degrees. The corresponding span angle of the circular curve S is r. The radius length and the center point of the circle are R and C, respectively. Besides, the length between the front wheels and the rear wheels is a constant d. The length of the vehicle affects the length of the radius. The radius length R is obtained as follows:

$$R = d / \sin\delta. \quad (6)$$

In addition, according to the characteristic of a circle, the angle r and the secant P are obtained respectively as follows:

$$r = S / R, \text{ and} \quad (7)$$
$$P = R\sqrt{2(1-\cos r)}. \quad (8)$$

Whenever the vehicle moves along a certain trajectory, the line in the direction of the front wheels is a tangent of the trajectory of the vehicle. As illustrated in Fig. 4, we obtain

$$\omega + u + \sigma = \pi/2, \quad (9)$$

and

$$\delta + \omega + u = \pi/2. \quad (10)$$

Besides, the three points O, B and C compose an equilateral triangle in which the distance from O to C and that from B to C are both just the radius of the circle, so

$$u + \sigma = (\pi - r)/2 = \pi/2 - r/2. \quad (11)$$

By substituting (11) into (9), we obtain

$$\omega = \pi/2 - (u + \sigma) = r/2. \quad (12)$$

By substituting (12) into (10), we obtain

$$u = \pi/2 - \delta - \omega = \pi/2 - \delta - r/2. \quad (13)$$

Now, the coordinates x and y of the location B can be obtained by substituting (6), (7), (8) and (13) into Equations (4) and (5). The results are as follows:

$$\begin{aligned} x = P\cos u &= R\sqrt{2(1-\cos r)}\cos\left(\frac{\pi}{2}-\delta-\frac{r}{2}\right) \\ &= \frac{d}{\sin\delta}\sqrt{2\left(1-\cos\frac{S}{R}\right)}\cos\left(\frac{\pi}{2}-\delta-\frac{S}{2R}\right) \\ &= \frac{d}{\sin\delta}\sqrt{2\left(1-\cos\frac{S\sin\delta}{d}\right)}\cos\left(\frac{\pi}{2}-\delta-\frac{S\sin\delta}{2d}\right), \end{aligned} \quad (14)$$

$$\begin{aligned} y = P\sin u &= R\sqrt{2(1-\cos r)}\sin\left(\frac{\pi}{2}-\delta-\frac{r}{2}\right) \\ &= \frac{d}{\sin\delta}\sqrt{2\left(1-\cos\frac{S}{R}\right)}\sin\left(\frac{\pi}{2}-\delta-\frac{S}{2R}\right) \\ &= \frac{d}{\sin\delta}\sqrt{2\left(1-\cos\frac{S\sin\delta}{d}\right)}\sin\left(\frac{\pi}{2}-\delta-\frac{S\sin\delta}{2d}\right), \end{aligned} \quad (15)$$

where

$$S = v * t. \quad (16)$$

In Equations (14) and (15), the values of x and y are functions of d, S and δ. The value d is a constant. The value S is the product of the vehicle speed v and the unit time t. The unit time is assumed to be a constant. Hence, by substituting (16) into Equations (14) and (15), x and y can be modified as functions of δ and v to be

$$x = f(\delta, v), \quad (17)$$

and

$$y = g(\delta, v). \quad (18)$$

According to the formula of the coordinates x and y in the next time instant in Equations (17) and (18), the location that satisfies the second visual contact constraint can be calculated in the following. As shown in Fig. 5, when the front wheels of the vehicle turns δ degrees and arrives at the location B by traveling a circular curve, the direction vector v_2 of the front wheels is that of the tangent of the circular curve. The vector from the location B to the person's position P is assumed to be v_1. The angle between v_1 and v_2 is assumed to be θ. When the angle θ is equal to the angle δ, the direction v_1 is the same as that of the vehicle head. The angle of θ will be the angle between the direction of the vehicle head and that of the front wheels of the vehicle in the next time instant so that the second visual contact constraint is satisfied. Hence, the question is simplified to obtain the location B and the turning angle δ so that the following function is satisfied:

$$h(\theta, \delta) = \theta - \delta = 0. \quad (19)$$

In the following, the derivation of the angle of θ is elaborated. The angle θ can be calculated according to the inner product of the vectors v_1 and v_2. Assume that the coordinates of points B and P are (x, y) and (x_1, y_1), respectively. Then, the vector v_1 is

$$v_1 = (x_1 - x, y_1 - y). \quad (20)$$

The coordinates of the point B are generated using Equations (17) and (18). The coordinates of the point P are generated by computer vision techniques in real time and assumed to be known in this study. The direction vector v_2 of the front wheels of the vehicle in the next time instant is calculated according to the characteristic of the tangent of the trajectory and described in the following. As shown in Fig. 6, the vector v_3 whose length is that of the radius R begins from the location B to the rotation center C of the circular curve. The vector v_2 can be calculated according to the inner product of v_2 and v_3 as follows:

$$v_2 \cdot v_3 = 0. \quad (21)$$

The vector v_2 is calculated according to the vector v_3, so the vector v_3 has to be calculated first. The coordinates x_c and y_c of the rotation center C are affected by the turning angle of the wheels and the length of the vehicle, and are obtained as follows:

$$(x_c, y_c) = (R\cos\delta, -d). \quad (22)$$

Because the formula of R is given in Equation (6), the coordinates x_c and y_c can be rewritten as

$$(x_c, y_c) = (d\cos\delta/\sin\delta, -d) = (d\cot\delta, -d). \quad (23)$$

Hence, according to the coordinates of points B and C in Equations (17), (18) and (23), the vector v_3 from point B to point C is derived as follows:

$$v_3 = (d\cot\delta\text{-}x,\ \text{-}d\text{-}y). \tag{24}$$

Moreover, because the inner product of v_2 and v_3 is zero in Equation (21), the vector v_2 is obtained as follows:

$$v_2 = (d\text{+}y,\ d\cot\delta\text{-}x). \tag{25}$$

Now the formula of the vector v_1 and v_2 have been derived and shown in Equations (20) and (25). The angle θ between the direction vectors v_1 and v_2 shown in Fig. 5 is calculated by the following formula of the inner product:

$$v_1 \cdot v_2 = |v_1| \cdot |v_2| \cdot \cos\theta. \tag{26}$$

Hence,

$$\theta = \operatorname{acos}\left(\frac{v_1 \cdot v_2}{|v_1| \cdot |v_2|}\right) = \operatorname{acos}\left(\frac{(x_1 - x)\cdot(d + y) + (y_1 - y)\cdot(d\cot\delta - x)}{\sqrt{(x_1 - x)^2 + (y_1 - y)^2}\cdot\sqrt{(d + y)^2 + (d\cot\delta - x)^2}}\right) \tag{27}$$

Because x and y are the functions of δ and v in Equations (17) and (18), the angle θ can be calculated according to the variables δ and v. The formula of the angle of θ can be written as a function G as follows:

$$\theta = \operatorname{acos}\left(\frac{v_1 \cdot v_2}{|v_1| \cdot |v_2|}\right) = G(\delta, \mathrm{v}). \tag{28}$$

Hence, The function h in Equation (19) can be modified as a function H of δ and v in the following:

$$H(\delta, v) = h(\theta, \delta) = G(\delta, v) - \delta = 0. \tag{29}$$

According to the function H in Equation (29), a proper turn angle δ can be generated using an iteration method when the speed v of the vehicle is given. The approach used in this study to obtain the speed v of the vehicle is introduced in Section 5. Hence, when the function (29) is satisfied according to a calculated δ and a given v, the position of the vehicle in the next time instant will satisfy the second visual contact constraint and the circular curve will be a proper navigation trajectory.

3.2. Proposed limiting distances satisfying the third visual contact constraint

Appropriate ranges for the distance bounds d_1 and d_2 in (3) which satisfy the second constraint are derived in the following. As shown in Fig. 7, d_1 is the nearest distance and d_2 is the farthest distance. These two values are calculated according to the relation between the visible area and the person-bounded area. The value d_1 is the smallest distance between the vehicle and the person to make the visible area totally cover the person-bounded area. d_1 can be computed using the condition that the two boundary lines of the visible area are both the tangents of the person-bounded area. The distance d_1 is derived in terms of the person's speed v_p, the unit time t, and the visual angle 2α of the camera. Because the person's next position must be located inside the person-bounded area, the distance $v_p t$ that the person walks in a unit time must be smaller than the radius of the person-bounded area, that is,

$$v_p t \le |\overline{P_i T}|, \tag{30}$$

where P_i and $|\overline{P_i T}|$ are the center and the radius of the person-bounded area, respectively. Because P_i, T, and B_{i+1} form a right triangle and $|\overline{P_i B_{i+1}}|$ is the longest border of the triangle, we have

$$|\overline{P_i T}| = |\overline{P_i B_{i+1}}| \cdot \sin\alpha \cdot \tag{31}$$

According to (30) and (31), we obtain

$$v_p t / \sin\alpha \le |\overline{P_i B_{i+1}}|, \tag{32}$$

where $d_1 = v_p t/\sin\alpha$ and $D(B_{i+1}, P_i) = |\overline{P_i B_{i+1}}|$.

Because the proposed visible area is a triangle, the border of the triangle that is perpendicular to the direction of the vehicle head is called the farthest boundary of the visible area. As shown in Fig. 7(b), when the farthest boundary of the visible area is the tangent of the person-bounded area, the distance d_2 can be calculated. Assume that the distance from the farthest boundary of the visible area to the position of the vehicle is y_{max}. $y_{max} - |\overline{P_i B_{i+1}}|$ is the radius of the person-bounded area and is bigger than or equal to the distance $v_p t$. That is,

$$v_p t \le y_{max} - |\overline{P_i B_{i+1}}|, \tag{33}$$

which can be rewritten as

$$|\overline{P_i B_{i+1}}| \le y_{max} - v_p t, \tag{34}$$

where $d_2 = y_{max} - v_p t$ and $D(B_{i+1}, P_i) = |\overline{P_i B_{i+1}}|$.

The value y_{max} may be derived in terms of the maximum speed V_{max} of the vehicle, the maximum turn angle A_{max} of the front wheels, and the visual angle 2α of the camera. According to Equation (25), the direction vector v_2 of the front wheels at position B, as shown in Fig. 8, is derived as

$$v_2 = (d\text{+}y_b,\ d\cot(A_{max})\text{-}x_b), \tag{35}$$

where x_b and y_b are the coordinates of the vehicle at position B, A_{max} is the maximum turn angle of the vehicle, and d is the distance between the front and the rear wheels of the vehicle. The coordinates x_b and y_b are derived from the maximum turn angle A_{max} of the front wheels and the maximum speed V_{max} of the vehicle in Equations (17) and (18), and can be written as two functions:

$$x_b = f(A_{max}, V_{max}), \tag{36}$$

$$y_b = g(A_{max}, V_{max}). \tag{37}$$

When the direction vector v_2 of the front wheels is calculated, the direction vector v_4 of the vehicle head can be obtained since the angle between v_2 and v_4 is A_{max}. The vector v_4 is derived as follows:

$$v_4 = (x_4, y_4) = v_2 \cdot \begin{bmatrix} \cos A_{max} & \sin A_{max} \\ -\sin A_{max} & \cos A_{max} \end{bmatrix}. \tag{38}$$

The equation of the line with the vector v_4 passing through the point B is written as

$$\mathrm{L4}: \frac{y_4}{x_4}x + \left(y_b - \frac{y_4}{x_4}x_b\right) - y = 0. \tag{39}$$

Besides, the angle between the right boundary line L5 of the visible area and the direction of the vehicle head is α.

Hence, the line equation of L5 is

$$\mathrm{L5}: x(\cot\alpha) - y = 0. \quad (40)$$

According to Equations (39) and (40), the coordinates, x_{max} and y_{max}, of the intersection point corresponding to L4 and L5 are obtained as follows:

$$x_{max} = \frac{y_b x_4 - y_4 x_b}{(\cot\alpha)x_4 - y_4} \text{ and } y_{max} = \frac{(\cot\alpha)(y_b x_4 - y_4 x_b)}{(\cot\alpha)x_4 - y_4}. \quad (41)$$

According to (32), (34) and (41), the third constraint can be rewritten as

$$v_p t / \sin\alpha \le D(B_{i+1}, P_i) \le \frac{(\cot\alpha)(y_b x_4 - y_4 x_b)}{(\cot\alpha)x_4 - y_4} - v_p t. \quad (42)$$

In Equation (42), the values of the upper bound d_2 and the lower bound d_1 of the distance in the third visual contact constraint are obtained. When the ALV navigates in a mean time, this constraint is a condition of the derivation of the trajectory that satisfies the second visual contact constraint. According to this constraint, the distance between the next position, derived by the formula of the trajectory in the above section, of the vehicle and the person's current position can not be nearer than the lower bound d_1 . The relation between the proposed formulas in Sections 3.2 and 3.3 that satisfy three visual contact constraints is derived in two theorems in the next section. These two theorems prove that the three visual contact constraints based on the proposed formulas can be correctly achieved in the successional navigation. Using the result of the theorem, an algorithm proposed in Section 5 makes the ALV achieve the robust navigation so that the person will always appear in the image.

4. Analysis of the Visual Contact Constraints

In this section, two properties are derived from an analysis of the visual contact constraints proposed in Section 2.2. The first property, derived from the first and the second constraints in (1) and (2), confirms that the direction of the vehicle head at the next position points straightly forward to the person's current position. The second property, derived from all three constraints, confirms that the person at the next position must appear in the image that is captured from the next position of the vehicle. When the second property is satisfied in the navigation stage, the vehicle will robustly follow the walking person ahead. If the person at cycle i appears in the captured image and the vehicle at cycle i+1 can capture the image of the person, the vehicle can capture the image of the person at cycle i+2, i+3, i+4…etc. In the following, we first define some symbols, followed by the details of the derivations of the properties.

Definitions of symbols:

- B_i : the position of the vehicle at cycle i;
- P_i : the position of the person at cycle i;
- V_i : the speed of the vehicle at cycle i;
- A_i : the turn angle of the front wheels of the vehicle at cycle i;
- v_p : the detected speed of the person at cycle i;
- $L(B_i)$: the location of the vehicle at cycle i;
- $L(P_i)$: the location of the person at cycle i;
- $D(B_i, P_i)$: the distance between B_i and P_i at cycle i;
- $A(B_i, P_i)$: the angle between $\overrightarrow{B_i P_i}$ and the direction of the vehicle head;
- V_{max}: the maximum speed of the vehicle;
- A_{max}: the maximum turn angle of the front wheels of the vehicle;
- t: the interval time between two sampling instants;
- 2α: the visual angle of the camera;
- S_i: the distance that the vehicle travels in a speed V_i and a unit time t;
- R: the radius length when the vehicle travels by turning δ degrees;
- (x_i, y_i): the coordinates of the vehicle B_i that navigates using the turn angle A_i and the speed V_i in a unit time t from the position B_{i-1};
- (x_b, y_b): the coordinates of the vehicle that navigates using the turn angle A_{max} and the speed V_{max} in a unit time t;
- $\overline{\mathrm{L4}}_{x_i, y_i}$: the line equation that passes through the coordinates (x_i, y_i) and possesses the same direction vector of the vehicle head;
- L4: the line equation that passes through the coordinates (x_b, y_b) and possesses the same direction vector of the vehicle head;
- Region 1: the area in which P_i satisfies $A(B_i, P_i) \le \alpha$, $V_i t + v_p t / \sin\alpha \le D(B_i, P_i)$ and $\mathrm{L4}(P_i) \le 0$;
- Region 2: the area in which P_i satisfies $A(B_i, P_i) \le \alpha$, $V_i t \le D(B_i, P_i) \le V_i t + v_p t / \sin\alpha$ and $\mathrm{L4}(P_i) \le 0$;
- φ : the angle between the line L4 at the position B_i and the direction of the vehicle head at the position B_{i-1}.

The following theorem proposes the condition of the trajectory that satisfies the second visual contact constraint. If the condition is satisfied, a proper trajectory can be derived so that the direction of the vehicle head at the next position straightly points forward to the person's current position. In this theorem, one condition is that the distance between the vehicle and the person must be farther than the navigation distance of the vehicle in the unit time. If this condition is not satisfied, the next position of the vehicle will be in front of the person's position so that the second visual contact constraint must not be satisfied. Another condition in this theorem considers the capability, the maximum speed and the maximum turn angle, of the vehicle. The person needs be located in the region 1 or the region 2 so that the second visual contact constraint can be satisfied when the vehicle navigates under the maximum speed and the maximum turn angle in the unit time. The condition in Theorem 1 is a general case. When a half of the visual angle is smaller than the angle φ, Corollary 1 based on Theorem 1 is proposed.

Theorem 1. In Fig. 9, if $V_i t \le D(B_i, P_i)$ is true, B_i is at the original point, and P_i is in Region 1 or Region 2, the constraint $A(B_{i+1}, P_i) = 0$ is true.

Proof:

In this study, we assume that $S_i \le \pi R/2$. That is, the navigation distance of the vehicle is not farther than a quarter of the circumference that is formed by the circular trajectory of the vehicle. According to the coordinates x_i and y_i of the vehicle in Equations (14) and (15), x_i and y_i are monotonically increasing when S_i increases. Besides, S_i is continue when we assume V_i is continue in Equation (16). Hence, when we assume that

$$V_1 \le V_2, \quad (1.1)$$

V_1 can be assigned as zero and V_2 is assigned as V_{max}. As shown in Fig. 9, when the vehicle navigates using the turn angle A_{max}, we can obtain the corresponding positions O and B to the speed V_1 and V_2, respectively. When the person's position P_i is in Region 1 or Region 2, two conditions are satisfied as follows:

$$\overline{\mathrm{L4}}^{0,0}(P_i) > 0 \text{ and } \overline{\mathrm{L4}}^{x_b, y_b}(P_i) < 0 \quad (1.2)$$

When the relation between V_1 and V_2 is obtained, we will prove that a speed V_i must be found so that its

corresponding coordinates x_i and y_i satisfy the following relation:

$$\overline{\mathrm{L4}}_{x_i,y_i}(P_i)=0. \tag{1.3}$$

At first, we can assume that a value of the speed V is between V_1 and V_2, and written as follows:

$$V_1 \le V \le V_2. \tag{1.4}$$

The corresponding coordinates of the position of the vehicle to the speed V are noted as x and y. According to Equation (1.4), the speed V can be assigned as follows:

$$V=\frac{V_1+V_2}{2}. \tag{1.5}$$

Hence, the speed V_1 and V_2 can be reassigned using the following equation:

$$\begin{cases}\overline{\mathrm{L4}}_{x,y}(P_i)>0 \rightarrow V_1=V, \\ \overline{\mathrm{L4}}_{x,y}(P_i)<0 \rightarrow V_2=V.\end{cases} \tag{1.6}$$

Because the speed V is continue, a speed V_i must be generated to satisfy the following equation when Equations (1.5) and (1.6) are executed recursively.

$$\overline{\mathrm{L4}}_{x,y}(P_i)=0 \rightarrow V_i=V. \tag{1.7}$$

Hence, the speed V_i is obtained to satisfy Equation (1.3). Besides, because the distance between the vehicle and the person satisfies the following condition

$$V_i t \le D(B_i,P_i), \tag{1.8}$$

the person's position P_i is guaranteed to be in front of the vehicle after a period of time t. We can guarantee the following equation be satisfied according to Equations (1.3) and (1.8).

$$A(B_{i+1},P_i)=0. \tag{1.9}$$

This completes the proof of Theorem 1.

The following corollary considers a situation that the angle α is smaller than the angle φ in Theorem 1. In this corollary, all positions in the region 1 and the region 2 can be pointed by the direction of the vehicle head when the vehicle navigates using the maximum speed and the maximum turn angle in the unit time. Hence, when all positions of the person satisfying the condition in Corollary 1, the trajectory satisfying the second visual contact constraint can be derived.

Corollary 1. If $A(B_i,P_i)\le\alpha$, $\varphi\ge\alpha$, and $V_i t \le D(B_i,P_i)$ all are true, the constraint $A(B_{i+1},P_i)=0$ is true.

Proof :

As shown in Fig. 10, for any person's position P_i, when the following condition is satisfied,

$$A(B_i,P_i)\le\alpha, \tag{1.10}$$

the position P_i will be located on the left side of L5 so that

$$\mathrm{L5}(P_i)\le 0. \tag{1.11}$$

Because the angle α is smaller than the angle φ, written as

$$\varphi\ge\alpha, \tag{1.12}$$

and the person's position P_i satisfies Equation (1.11), we can obtain the following condition as shown in Fig. 10.

$$\mathrm{L4}(P_i)\le 0. \tag{1.13}$$

When conditions (1.10), (1.13) and $V_i t \le D(B_i,P_i)$ are satisfied, the position P_i is confirmed to be in Region 1 or Region 2. According to Theorem 1, we obtain

$$A(B_{i+1},P_i)=0. \tag{1.15}$$

This completes the proof of Corollary 1. The following theorem proposes the condition of the robust navigation so that the next position of the person must be in the view of the camera at the next position of the vehicle. In this theorem, two conditions have to be satisfied. One is that the distance between the vehicle and the person needs be farther than the distance $V_i t$ proposed in Theorem 1 plus the lower bound d_1 in the third visual contact constraint. The other condition is that the person's position needs be located in Region 1. The first condition guarantees that the distance between the person's current position and the next position of the vehicle is still farther than the lower bound d_1 to satisfy the third visual contact constraint. The second condition like Theorem 1 considers the maximum speed and the maximum turn angle of the vehicle. The condition in Theorem 2 is a general case. If a half of the visual angle is smaller than the angle φ, Corollary 2 that is based on Theorem 2 is proposed.

Theorem 2. In Fig. 9, if $V_i t + v_p t/\sin\alpha \le D(B_i,P_i)$ is true, B_i is on original point, and P_i is in Region 1, the result $A(B_{i+1},P_{i+1})\le\alpha$ is satisfied.

Proof:

According to the following condition:

$$V_i t + v_p t/\sin\alpha \le D(B_i,P_i), \tag{2.1}$$

we can obtain another equation as follows:

$$V_i t \le D(B_i,P_i). \tag{2.2}$$

According to Equation (2.2) and Theorem 1, the second visual contact constraint can be satisfied and written as

$$A(B_{i+1},P_i)=0. \tag{2.3}$$

In addition, the distance between the positions of the vehicle in the next time instant and in the current time instant is smaller than $V_i t$. The condition is written as follows:

$$L(B_{i+1})-L(B_i)=D(B_{i+1},B_i)\le V_i t \tag{2.4}$$

The condition (2.1) can be rewritten in the following.

$$L(P_i)-L(B_i)=D(B_i,P_i)\ge V_i t + v_p t/\sin\alpha. \tag{2.5}$$

When (2.5) subtracts (2.4), we obtain

$$L(P_i)-L(B_{i+1})=D(B_{i+1},P_i)\ge v_p t/\sin\alpha. \tag{2.6}$$

According to Equations (2.3) and (2.6), the person-bounded area of P_i is totally covered by the visible area of B_{i+1}. Hence, the person's (i+1)th position is located inside the visible area of B_{i+1} and the formula is written as

$$A(B_{i+1},P_{i+1})\le\alpha. \tag{2.7}$$

This completes the proof of Theorem 2. The following corollary considers a situation that the angle α is smaller than the angle φ in Theorem 2. In this corollary, all positions in the region 1 can be pointed by the direction of the vehicle head when the vehicle navigates using the maximum speed and the maximum turn angle in the unit time. Hence, when all positions of the person in the view of the current position of the vehicle, the first visual contact constraint is satisfied. All conditions in Corollary 2 satisfy the condition of Corollary 1 so that the second visual contact constraint is satisfied. In addition, the condition of the distance in Corollary 2 satisfies the formula of the third constraint. Hence, the trajectory that makes the next position of the person must be in the view of the camera at the next position of the vehicle can be derived.

Corollary 2. If $A(B_i, P_i) \le \alpha$, $\varphi \ge \alpha$, and $V_i t + v_p t / \sin\alpha \le D(B_i, P_i)$ all are true, the result $A(B_{i+1}, P_{i+1}) \le \alpha$ is satisfied.

Proof :

As shown in Fig. 10, for any person's position P_i, when the following condition is satisfied,

$$A(B_i, P_i) \le \alpha, \tag{2.8}$$

the position P_i will be located on the left side of L5 so that

$$\mathrm{L5}(P_i) \le 0. \tag{2.9}$$

Because the angle α is smaller than the angle φ, written as

$$\varphi \ge \alpha, \tag{2.10}$$

and the person's position P_i satisfies Equation (2.9), we can obtain the following condition as shown in Fig. 10.

$$\mathrm{L4}(P_i) \le 0. \tag{2.11}$$

When conditions (2.8), (2.11) and $V_i t + v_p t / \sin\alpha \le D(B_i, P_i)$ are satisfied, the position P_i is confirmed to be in Region 1. According to the condition that P_i is in Region 1 and $V_i t + v_p t / \sin\alpha \le D(B_i, P_i)$ in Theorem 2, we obtain

$$A(B_{i+1}, P_{i+1}) \le \alpha. \tag{2.13}$$

This completes the proof of Corollary 2. Two proposed theorems above show the robustness and the validity of the proposed trajectory. In addition, these two theorems prove the correctness of the proposed visual contact constraints. In Theorem 1, the condition of the person's position makes the derived trajectory satisfy the second visual contact constraint. This theorem is used in the proof of Theorem 2. In Theorem 2, the condition of the person's position makes the derivation of the trajectory satisfy the robust navigation so that the next position of the person must be in the view of the camera at the next position of the vehicle. Using the condition in Theorem 2, an upper bound of the speed of the vehicle can be derived. This bound of the speed is used in the proposed algorithm described in the next section so that the robust navigation can be achieved.

5. Proposed Trajectory Planning Algorithm

In this section, the proposed trajectory planning algorithm is described. Using the proposed algorithm, the control parameters, the turning angle, and the forward speed of the vehicle, which are required for vehicle guidance, are derived. Before introducing the algorithm, the derivation of the speed boundary of the vehicle is described in the following. In Theorem 2, the condition of the distance between B_i and P_i is derived and written as

$$V_i t + v_p t / \sin\alpha \le D(B_i, P_i) \tag{43}$$

Hence, the upper bound of the speed V_i of the vehicle is derived as follows:

$$V_i \le \frac{D(B_i, P_i) - v_p t / \sin\alpha}{t}. \tag{44}$$

When the speed of the vehicle is smaller than the upper bound, a lower bound of the speed is also need to be derived. When Equation (29) is satisfied to fit the second constraint in (2), the slower the speed, the bigger the turning angle, and vice versa. Because the turning angle of the front wheels of the vehicle possesses a maximum value A_{max} that is a constant, the speed of the vehicle is a minimum one to satisfy Equation (29). Hence, the lower bound V_l of the speed is derived by satisfying the following equation:

$$H(A_{max}, V_l) = G(A_{max}, V_l) - A_{max} = 0. \tag{45}$$

Hence, the speed of the vehicle is need to satisfy the condition as follows:

$$V_l \le V_i \le \frac{D(B_i, P_i) - v_p t / \sin\alpha}{t}. \tag{46}$$

Now, the trajectory planning algorithm is proposed as follows:

Trajectory Planning Algorithm:

Step 1. If the person P_i is in the image, calculate the person's speed v_p and location (x_1, y_1). Otherwise, stop the vehicle and go to Step 1.

Step 2. Calculate the distance D between the person's position P_i and the position B_i of the vehicle.

Step 3. Calculate the lower bound V_l of the speed. The value V_l satisfies the following equation.

$$H(A_{max}, V_l) = G(A_{max}, V_l) - A_{max} = 0. \tag{47}$$

where A_{max} is a constant.

If $D(B_i, P_i) \le V_l \cdot t$ is true, stop the vehicle and go to Step 1. Otherwise, go to step 4.

Step 4. Calculate the upper bound V_u of the speed.

$$V_u = \frac{D(B_i, P_i) - v_p t / \sin\alpha}{t} = \frac{D(B_i, P_i)}{t} - \frac{v_p}{\sin\alpha}. \tag{48}$$

Step 5. Calculate the speed V_i of the vehicle according to the person's speed v_p, V_u and V_l.

If $V_u \le V_l$ is true, the speed V_l is assigned as V_l. Otherwise,

$$\begin{aligned} v_p \le V_l &\Rightarrow V_i = V_l, \\ V_l \le v_p \le V_u &\Rightarrow V_i = V_p, \\ v_p \ge V_u &\Rightarrow V_i = V_u. \end{aligned}$$

Step 6. Calculate the turn angle δ of the vehicle according to the given speed V_i of the vehicle.

The angle δ satisfies the following equation and is calculated by the iteration method.

$$H(\delta, V_i) = G(\delta, V_i) - \delta = 0. \tag{49}$$

Step 7. Send control parameters V_i and δ to the vehicle.

Step 8. Go to step 1.

6. Experimental Results

The proposed method has been implemented and used to steer a real ALV to follow a person, as shown in Fig. 11. In our experiments, the width and the length of the ALV are 40 cm and 120 cm, respectively. The length between the front wheels and the rear wheels of the ALV is 82 cm. The maximum speed V_{max} of the vehicle is 80 cm/sec. The maximum turn angle A_{max} of the front wheels of the vehicle is 30 degrees to the right or to the left. The interval time t between two sampling instants is 1.5 sec. The lens and the visual angle 2α of the camera used to capture the image of the person are 8mm and 50 degrees, respectively. The approach used in this study to obtain the person's location in the vehicle coordinate system by calculating three-dimensional coordinates of the rectangle shape that is attached on the person's shirt is described in [1]. The structure of the vehicle system is introduced in detail in [23].

Figs. 12 through 14 show images in our experiments of guiding the ALV to navigate in a building corridor using the trajectory planning algorithm. Every figure includes two photographs that are captured by the camera mounted on the vehicle. The two photographs are grabbed when the ALV navigates before and after applying the proposed algorithm, respectively. As shown in Fig. 12(a) and Fig. 13(a), the person's positions, (-54.81, 193.16) and (76.43,110.12), are near the left and the right boundary line, respectively, of the camera. The person will be out of the camera view if the vehicle keeps navigating in the straight direction. According to the calculation of the proposed algorithm, the speed of the vehicle and the turn angle of the front wheels in Fig. 12 and Fig. 13 are 14.60 cm/sec and -35 degrees, and 29.60 cm/sec and 35 degrees, respectively. As shown in Fig. 12(b) and Fig. 13(b), the vehicle stably keeps the visual contact with the person. Fig. 14 shows an experimental example that the person is near the straight direction of the vehicle head. The speed of the vehicle and the turn angle of the front wheels are 18.85 cm/sec and –4 degrees. The vehicle just needs adjust a small angle of the front wheels to keep the visual contact with the walking person. Besides, the derived speed of the vehicle still makes the distance between the vehicle and the person in a reasonable range. An example of a sequence of experimental images in a real indoor environment is shown in Fig. 15. In Fig. 16, a sequence of images shows that the person turns to the left in the corridor. These two figures show the robustness of the proposed trajectory so that the vehicle keeps the visual contact with the person in the successional navigation.

7. Conclusions

In this study, a robust trajectory planning method has been proposed so that the person must appear in the image when the ALV follows the walking person ahead. This goal is achieved when three visual contact constraints based on the visual field model are satisfied. The main contributions in this study are that the visual contact constraints are formulated, a visual filed model is proposed, and a robust trajectory planning algorithm is derived. In the visual field model, a visible area and a person-bounded area are proposed. Using the relation of these two areas, three visual contact constraints are proposed to guarantee that the person-bounded area is totally covered by the visible area all the time. This means that the person can appear in the captured image all the time. According to the visual contact constraints, the formula of the trajectory of the ALV and the limit in deriving the trajectory are proposed. Based on the derived condition, two theorems are proposed to show the robustness and the validity of the trajectory. In addition, these two theorems prove the correctness of the proposed visual contact constraints. Finally, the algorithm of the trajectory planning for ALV guidance is proposed to obtain control parameters of the ALV. In the experiments, this approach is implemented on a real ALV, and successful navigation sessions confirm the feasibility and robustness of the approach.

References

[1] C. H. Ku and W. H. Tsai, "Smooth Autonomous Land Vehicle Navigation in Indoor Environments by Person Following Using Sequential Pattern Recognition, Fuzzy Speed Control and Computer Vision Techniques," *Proceedings of the Joint Conference of the Fifth International Conference on Automation Technology and 1998 International Conference of Production Research* (*Asia Meeting*), Grand Hotel, Taipei, Taiwan, Republic of China, pp. 115, 20-22 July, 1998.

[2] R. M. Murray and S. S. Sastry, "Nonholonomic motion planning: steering using sinusoids," *IEEE Transaction on Automatic Control,* vol. 38, no. 5, pp. 700-716, 1993.

[3] M. S. Chang, P. Y. Ku, L. L. Wang, and W. H. Tsai, "Indoor autonomous land vehicle guidance by line following using computer vision techniques," *Proceedings of 1989 Workshop on Computer Vision, Graphics, and Image Processing*, Taipei, Taiwan, Republic of China, pp. 135-144, 1989.

[4] B. Matthews, M. Ruthemeyer, D. Perdue, and E. L. Hall, "Line following for a mobile robot," *Proceedings of the SPIE - The International Society for Optical Engineering*, Vol. 2588, pp. 610-617, 1995.

[5] W. J. Ke and W. H. Tsai, "Indoor autonomous land vehicle guidance by corner tracking using computer vision," *Proceedings of 1991 Workshop on Computer Vision, Graphics and Image Processing*, Tainan, Taiwan, Republic of China, pp. 133-139, 1991.

[6] Y. M. Su and W. H. Tsai, "Autonomous land vehicle guidance for navigation in buildings by computer vision, radio, and photoelectric sensing techniques," *Journal of the Chinese Institute of Engineers,* Vol. 17, No.1, pp. 63-73, 1994.

[7] H. I. Christensen, N. O. Kirkeby, S. Kristensen, L. Knudsen, and E. Granum, "Model-driven vision for indoor navigation," *Robotics and Autonomous Systems*, Vol. 12, No. 3-4, pp. 199-207, 1994.

[8] L. L. Wang, P. Y. Ku, and W. H. Tsai, "Model-based guidance on the longest common subsequence algorithm for indoor autonomous vehicle navigation using computer vision," *Automation in Construction*, Vol. 2, No. 2, pp. 123-137, 1993.

[9] T. Fukuda, S. Ito, N. Oota, F. Arai, Y. Abe, K. Tanaka, and Y. Tanaka, "Navigation system based on ceiling landmark recognition for autonomous mobile robot," *Proceedings of the IECON. International Conference on Industrial Electronics, Control, and Instrumentation*, Vol. 3, pp. 1466-1471, 1993.

[10] Gilg and G. Schmidt, "Landmark-oriented visual navigation of a mobile robot," *IEEE Transactions on Industrial Electronics*, Vol. 41, No. 4, pp. 392-397, 1994.

[11] C. Thrope, M. H. Hebert, T. Kanade, and S. A. Shafer, "Vision and navigation for Carnegie-Mellon NAVLAB," *IEEE Transactions on Pattern Analysis and Machine Intelligence*, Vol. 10, No. 3, pp. 362-373, 1988.

[12] J. D. Crisman and C. E. Thorpe, "SCARF: A color vision system that tracks roads and intersections," *IEEE Transactions on Robotics and Automation*, Vol. 9, No. 1, pp. 49-58, 1993.

[13] K. I. Kim, S. Y. Oh, S. W. Kim, H. Jeong, J. H. Han, C. N. Lee, B. S. Kim, and C. S. Kim, "An autonomous land vehicle PRV II: progresses and performance enhancement", *Proceedings of the Intelligent Vehicles '95. Symposium,* Detroit, MI, U.S.A., pp. 264-269, 1995.

[14] M. Schwarzinger, T. Zielke, D. Noll, M. Brauckmann, and W. von Seelen, "Vision-based car-following: detection, tracking, and identification", *IEEE Intelligent Vehicles Symposium,* pp. 24-29, 1992.

[15] K. Matsuda, M. Kamihira, M. Onchi, and T. Furukawa, "Design and implementation of tracking control system of autonomous mobile robot with multiple sensors," *Reports of the Faculty of Science and Engineering, Saga University*, Vol. 24, No. 1, pp. 73-82, 1995.

[16] U. D. Hanebeck and G. Schmidt, "A new high performance multisonar system for fast mobile robots,"

IROS. Proceedings of the IEEE/RSJ/GI International Conference on Intelligent Robots and Systems. Advanced Robotic Systems and the Real World, Vol. 3, pp. 1853-1860, 1994.
[17] H. Mori and M. Sano, "A guide dog robot Harunobu-5 - following a person," Proceedings IROS. IEEE/RSJ International Workshop on Intelligent Robots and Systems. Intelligence for Mechanical Systems, Vol. 1, pp. 397-402, 1991.
[18] O. Masoud and N. P. Papanikolopoulos, "Robust pedestrian tracking using a model-based approach," *Proceedings of IEEE Conference on Intelligent Transportation Systems*, Boston, MA, U.S.A.. 9-12 Nov., pp. 338-343, 1997.
[19] J. Denzler and H. Niemann, "Real-time pedestrian tracking in natural scenes," *Proceedings of 7th International Conference on Computer Analysis of Images and Patterns*, Berlin, Germany, 10-12 Sept., pp. 42-49, 1997.
[20] L. Trassoudaine, S. Jouannin, J. Alizon and J. Gallice, "Tracking systems for intelligent road vehicles," *International Journal of Systems Science*, Vol. 27, No. 8, pp. 731-743, 1996.
[21] V. F. Munoz and A. Ollero, "Smooth trajectory planning method for mobile robots," Proceedings of Conference on Computational Engineering in Systems Applications, pp. 700-705, Lille, France, 9-12 July, 1996.
[22] Z. Shiller and W. Serate, "Trajectory planning of tracked vehicles," *Journal of Dynamic Systems Measurement and Control-Transactions of the ASME*, Vol. 117, no.4, pp. 619-624, 1995.
[23] C. H. Ku, and W. H. Tsai, "Obstacle Avoidance for Autonomous Land Vehicle Navigation in Indoor Environments by Quadratic Classifier," *IEEE Transactions on Systems, man, and Cybernetics*, Vol. 29: Part B, No. 3, June 1999.

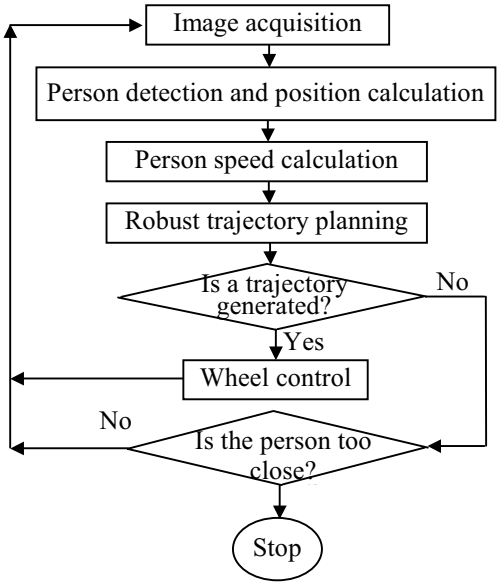

Figure 1. System flowchart.

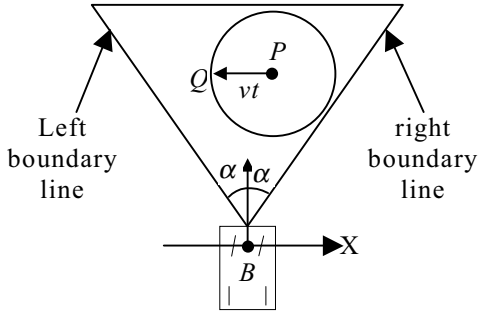

Fig. 2. Illustration of the visible area and the person-bounded area.

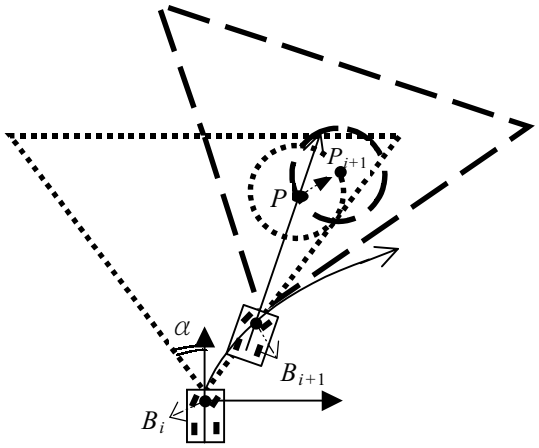

Fig. 3. Illustration of the positions *B* and *P* of the ALV and the person, respectively, at two time instants.

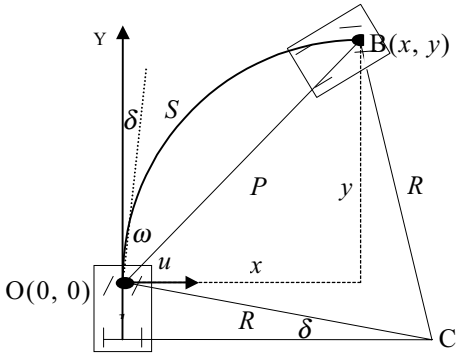

Fig. 4. Analysis of the path *S* on which the vehicle navigates from origin point O to location B by turning an angle of δ. The coordinates of location B are (*x*, *y*) in the VCS.

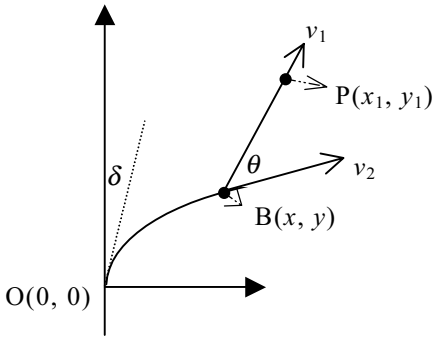

Fig. 5. Illustration of the relation between the position B of the vehicle and the position P of the person.

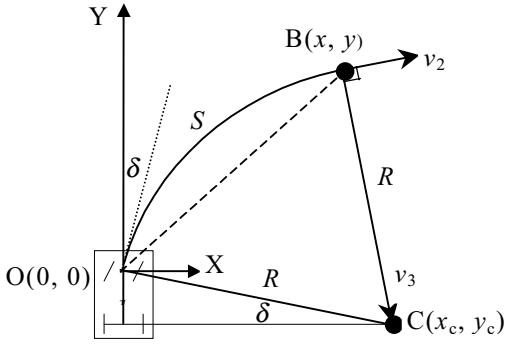

Fig. 6. Illustration of the positions of vectors v_2 and v_3. The angle between the vector v_2 and

the vector v_3 is rectangular.

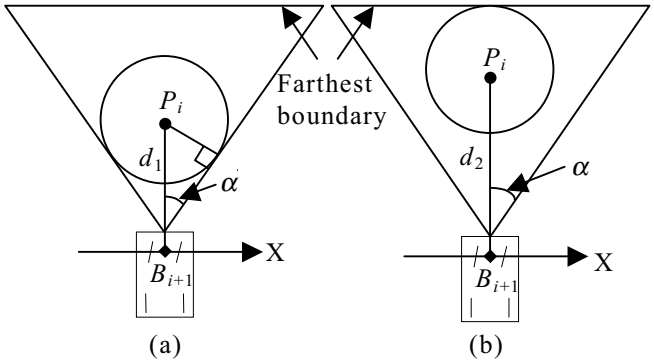

Fig. 7. Illustration of the bound of the distance between B_{i+1} and P_i in the third constraint. (a) The lower bound d_1. (b) The upper bound d_2.

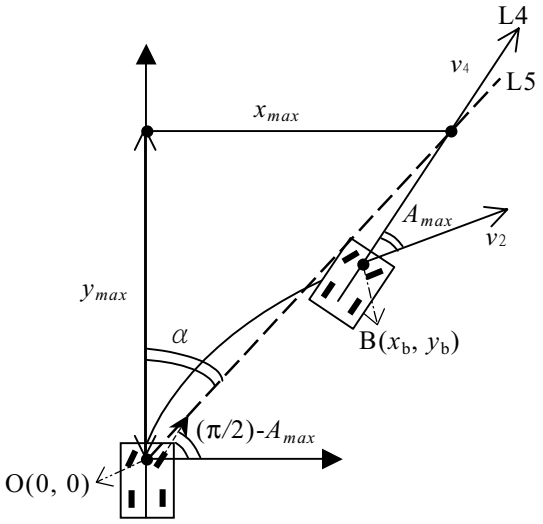

Fig. 8. The distance y_{max} of the visible area is derived by the maximum speed V_{max} of the vehicle, the maximum turn angle A_{max} of the front wheels, and the visual angle 2α of the camera.

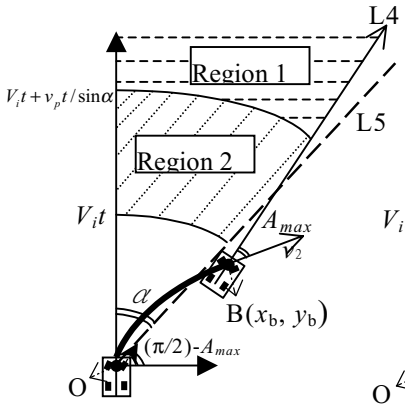

Fig. 9 Illustration of Region 1 and Region 2.

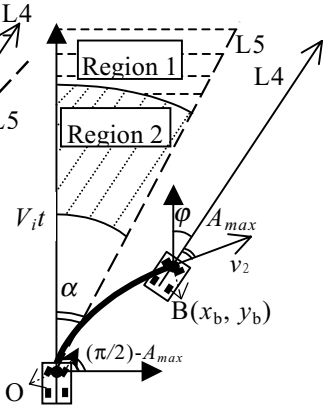

Fig. 10 Illustration of α and φ.

Fig. 11. The vehicle is guided automatically to follow a person who walks in front of the vehicle.

(a) (b)

Fig. 12. Illustration of the efficiency of applying the trajectory planning algorithm. (a) shows that the person's position is near the left boundary line of the camera. (b) shows the result of the ALV navigation.

(a) (b)

Fig. 13. Illustration of the efficiency of applying the trajectory planning algorithm. (a) shows that the person's position is near the right boundary line of the camera. (b) shows the result of the ALV navigation.

(a) (b)

Fig. 14. Illustration of the efficiency of applying the trajectory planning algorithm. (a) shows that the person's position is near the straight direction of the vehicle head. (b) shows the result of the ALV navigation.

Fig. 15. A sequence of experimental images in the corridor of a real indoor environment.

Fig. 16. The vehicle navigates to the left.